



# UNIVERSITÀ DI PARMA

## ARCHIVIO DELLA RICERCA

University of Parma Research Repository

Aggregates of polar dyes: beyond the exciton model

This is the peer reviewed version of the following article:

*Original*

Aggregates of polar dyes: beyond the exciton model / Anzola, Mattia; Painelli, Anna. - In: PHYSICAL CHEMISTRY CHEMICAL PHYSICS. - ISSN 1463-9076. - 23:(2021), pp. 8282-8291. [10.1039/D1CP00335F]

*Availability:*

This version is available at: 11381/2891700 since: 2023-06-11T07:47:16Z

*Publisher:*

Royal Society of Chemistry

*Published*

DOI:10.1039/D1CP00335F

*Terms of use:*

Anyone can freely access the full text of works made available as "Open Access". Works made available

*Publisher copyright*

note finali coverpage

(Article begins on next page)

# PCCP

Physical Chemistry Chemical Physics

Accepted Manuscript

This article can be cited before page numbers have been issued, to do this please use: M. Anzola and A. Painelli, *Phys. Chem. Chem. Phys.*, 2021, DOI: 10.1039/D1CP00335F.



This is an Accepted Manuscript, which has been through the Royal Society of Chemistry peer review process and has been accepted for publication.

Accepted Manuscripts are published online shortly after acceptance, before technical editing, formatting and proof reading. Using this free service, authors can make their results available to the community, in citable form, before we publish the edited article. We will replace this Accepted Manuscript with the edited and formatted Advance Article as soon as it is available.

You can find more information about Accepted Manuscripts in the [Information for Authors](#).

Please note that technical editing may introduce minor changes to the text and/or graphics, which may alter content. The journal's standard [Terms & Conditions](#) and the [Ethical guidelines](#) still apply. In no event shall the Royal Society of Chemistry be held responsible for any errors or omissions in this Accepted Manuscript or any consequences arising from the use of any information it contains.

Cite this: DOI: 00.0000/xxxxxxxxxx

Aggregates of polar dyes: beyond the exciton model<sup>†</sup>Mattia Anzola,<sup>a</sup> and Anna Painelli,<sup>\*a</sup>Received Date  
Accepted Date

DOI: 00.0000/xxxxxxxxxx

The physics of aggregates of polar and polarizable donor-acceptor dyes is discussed, extending a previous model to account for the coupling of electronic and vibrational degrees of freedom. Fully exploiting translational symmetry, exact absorption and fluorescence spectra are calculated for aggregates with up to 6 molecules. A two-step procedure is presented: in the first step, a mean-field solution of the problem is proposed to define the excitonic basis via a rotation of the electronic basis. The rotation is also accompanied by a Lang-Firsov transformation of the vibrational basis. In the second step, the aggregate Hamiltonian, written on the exciton basis, is diagonalized towards exact results. The procedure leads to a reduction of the dimension of the problem, since, at least for weak coupling, only states with up to 3 excitons are needed to get reliable results. More interestingly, the mean-field solution represents the proper reference state to discuss excitonic and ultraexcitonic effects. The emerging picture demonstrates that the exciton model offers a reliable description of aggregates of polar and polarizable dyes in the weak coupling regime, while ultraexcitonic effects are important in the medium-strong coupling regimes, and particularly so for J-aggregates where ultraexcitonic effects show up most clearly with multistability and multiexciton generation.

## 1 Introduction

Electrostatic intermolecular interactions are comparatively weak forces in supramolecular systems, but are responsible for energy transfer, an incoherent process where energy is transferred between different chromophores,<sup>1–4</sup> as well as for the coherent process of energy delocalization that governs the spectral properties of molecular crystals and aggregates.<sup>5–7</sup> Typically, energy transfer processes are investigated in loosely bound systems with intermolecular distances larger than  $\sim 10$  Å,<sup>8,9</sup> while in molecular crystals and aggregates fairly compact structures are of interest with intermolecular distances roughly comprised in the 3.5–7 Å range. In some systems, including molecular crystals as well as aggregates, intermolecular charge transfer (CT) interactions are important,<sup>10–13</sup> but here we will only discuss systems where CT interactions can be safely neglected, or, in other words, aggregates where electrons are localized in each molecular unit.<sup>5,6,14,15</sup>

The exciton model, widely adopted to describe optical spectra of molecular crystals and aggregates, dates back to the 60's<sup>5,14–16</sup> and found several successful applications, as recently extensively reviewed by Spano.<sup>7,17</sup> In the simplest version, it accounts for a single excitation on each molecule and, neglecting electrostatic

interactions among non-degenerate states, reduces the problem to that of a single particle, the exciton, moving on the molecular lattice. The corresponding problem is easily solved even on fairly large aggregates and, for symmetric (crystalline-like) systems, exact solutions in the thermodynamic limit are also available. Davydov splittings in crystals<sup>15</sup> and J and H-bands in aggregates<sup>14</sup> emerge quite naturally from this picture that can also be extended to discuss chiroptical properties of chiral aggregates.<sup>18–20</sup>

Molecules are flexible objects and their geometry usually responds to electronic excitations, as demonstrated by the prominent Frank-Condon structures often observed in molecular spectra. Extending the exciton model to account for molecular vibrations is non-trivial, mainly because the adiabatic (or Born-Oppenheimer) approximation cannot be applied. Indeed there are two easy limits: the vibrational frequency is either (a) much smaller or (b) much higher than the hopping frequency of the exciton. Case (a) corresponds to the adiabatic limit: the molecule has no time to relax its geometry following the exciton motion and vibrational coupling does not affect optical spectra. Case (b) corresponds to the antiadiabatic limit:<sup>21</sup> the exciton is trapped in the molecular site and the optical spectra show the same vibronic structure as the isolated molecule. Between these two limits the problem becomes non-adiabatic and special techniques must be adopted for its solution.<sup>17,22</sup> Quite interestingly, interpolating between the two limits, the vibronic structure observed in the aggregate can lead to a reliable estimate of the exciton delocalization, as first proposed by Spano.<sup>23</sup>

Neglecting the interactions between non-degenerate states, the

<sup>a</sup> Department of Chemistry, Life Science and Environmental Sustainability, University of Parma, 43124 Parma, Italy. E-mail: anna.painelli@unipr.it

<sup>†</sup> Electronic Supplementary Information (ESI) available: [Detailed derivation of the Hamiltonian in the exciton basis; additional computational results]. See DOI: 10.1039/cXCP00000x/

exciton model does not account for the effect of the local environment on the molecular properties, including e.g. the charge distribution in the ground or excited states, the transition energy and dipole moment etc. Typically, the parameters entering the exciton model, i.e. the reference transition frequency and the transition dipole moment, are obtained from the analysis of experimental data on isolated (solvated) molecules, thus implicitly accounting for environmental corrections. Indeed the environmental polarity has marginal effects in non-polar dyes, while the medium polarizability can be considered roughly constant organic media.<sup>24</sup> Extracting the same quantities from quantum chemical calculations in the gas phase is trickier. Most often reference transition frequencies are empirically adjusted.<sup>15,16</sup> Deviations from the exciton model are mainly recognized in the intensity of optical transitions as well as of CD spectra.<sup>25</sup> However, in aggregates of non-polar dyes with a large quadrupolar character large deviations from the exciton model are observed:<sup>26–30</sup> in these systems, the dense excitation spectrum at the molecular level, and the large molecular polarizability, make the approximations of the exciton model critical, with impressive effects on linear and non-linear optical spectra.

Even more intriguing is the situation in aggregates of polar dyes.<sup>31,32</sup> Indeed, as long as the molecular polarizability stays small, the exciton model, possibly with marginal corrections, still applies. However, in clusters of polar and polarizable dyes, typically push-pull dyes with large conjugation and hence strongly polarizable structures,<sup>33</sup> large deviations from the easy predictions of the exciton model are expected. Push-pull chromophores are  $\pi$ -conjugated molecules with an electron donor (D) and an acceptor (A) unit, whose low-energy physics is dominated by the charge resonance between a neutral DA (N) and a zwitterionic (Z)  $D^+A^-$  structure.<sup>34–36</sup> The resulting two state model accounts for both the molecular polarity and polarizability and very interesting physics emerges when clusters of dyes are considered, interacting via electrostatic intermolecular interactions. The model for interacting polar and polarizable dyes was introduced more than 40 years ago by Soos, as a toy model to describe the neutral-ionic phase transition in mixed stack CT crystals.<sup>37</sup> Multistability was recognized and discussed since then in different systems,<sup>38–40</sup> and spectroscopic effects in clusters of polar and polarizable molecules were also addressed.<sup>31,32,41–43</sup>

The number of basis states needed to describe aggregates of polar and polarizable dyes, increases as  $2^N$ ,  $N$  being the number of molecules. The relevant Hamiltonian can be diagonalized on fairly large systems.<sup>31</sup> Accounting for vibrational coupling however is challenging and so far exact solutions are only available for dimers,<sup>41</sup> while for larger systems, dramatic approximations have been introduced.<sup>42</sup> In a recent paper, Spano analyzed in detail absorption spectra of dimers of push-pull dyes fully accounting for vibrational coupling.<sup>43</sup> An interesting discussion of spectral badshapes emerges together with the demonstration of dramatic deviation from the Kasha behavior. In this paper we face the same problem, adopting the exciton transformation described in ref<sup>31</sup>, and a Lang-Firsov transformation for the vibrational coupling.<sup>21</sup> An optimized basis set with reduced dimension can then be defined, and, fully accounting for symmetry, we can handle com-

paratively large systems with up to 6 molecules. On a different perspective, the exciton transformation helps us to disentangle mean-field from excitonic and ultraexcitonic effects in these systems. Indeed, for weakly interacting aggregates, the Kasha model works well, provided the proper mean-field reference state is selected. On the other hand, in case of attractive interactions and strong coupling, multistability is expected and wild spectroscopic effects are observed, definitely beyond any exciton-like description.

## 2 The model

Each DA dye is described by two electronic diabatic states, corresponding to the two limiting neutral and zwitterion structures,  $|N\rangle$  and  $|Z\rangle$ , respectively (Fig. 1). The two electronic states are separated by an energy gap  $2z_0$  and are mixed by a matrix element  $-\tau$ . To account for the different geometry of the molecule in the two diabatic states, a single harmonic vibration with frequency  $\omega_v$  is considered on each molecular unit, leading to a linear dependence of the energy gap between the basis states on the coordinate, as shown by the diabatic potential energy curves in Fig. 1c.<sup>34</sup>

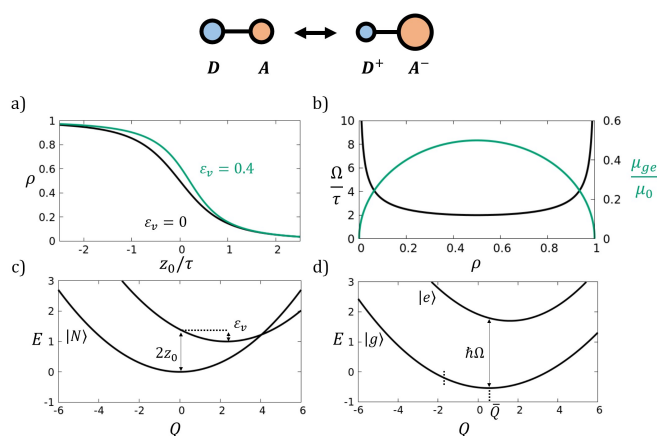


**Fig. 1** The isolated (gas-phase) dye. Top: the two resonating structures. (a) The  $\rho(z_0/\tau)$  curves calculated for  $\epsilon_v = 0$  and  $0.4 \tau$ . (b) the transition energy  $\Omega$  and the transition dipole moment as a function of  $\rho$ . (c) The potential energy surfaces for a system with  $\tau = 1$ ,  $\epsilon_v = 0.4$  and  $z_0 = 0.7$ . (d) the adiabatic PES calculated for the same system as in panel (c).

The Hamiltonian for an aggregate of  $N$  equivalent dyes, only interacting via electrostatic interactions, reads:

$$\mathcal{H} = \sum_i \left\{ \left[ 2z_0 - g(\hat{a}_i^\dagger + \hat{a}_i) \right] \hat{\rho}_i - \tau \sigma_i + \hbar \omega_v \left( \hat{a}_i^\dagger \hat{a}_i + \frac{1}{2} \right) \right\} + \sum_{i>j} V_{ij} \hat{\rho}_i \hat{\rho}_j \quad (1)$$

where  $i$  and  $j$  run on the molecular sites. The terms in the curly bracket define the molecular Hamiltonian and  $\hat{\rho}_i = |Z\rangle_i \langle Z|_i$  measures the weight of the zwitterionic state in the  $i$ -th molecule,  $\hat{\sigma}_i = |Z\rangle_i \langle N|_i + |N\rangle_i \langle Z|_i$ , and  $\hat{a}_i$  is the destruction operator for a vibrational quantum on the  $i$ -th molecule, so that the vibrational

coordinate and its conjugated momentum are:

$$\begin{aligned} Q_i &= \sqrt{\frac{\hbar}{2\omega_v}}(\hat{a}_i^\dagger + \hat{a}_i) \\ P_i &= i\sqrt{\frac{\hbar\omega_v}{2}}(\hat{a}_i^\dagger - \hat{a}_i) \end{aligned} \quad (2)$$

Finally,  $g$  is the electron-vibration coupling constant, related to the vibrational relaxation energy as  $\varepsilon_v = g^2/(\hbar\omega_v)$ , as shown in Fig. 1c. Specifically  $\varepsilon_v$  measures the energy gained by the molecule due to its geometrical rearrangement when its state changes from  $N$  to  $Z$ . The last term in the above equation accounts for intermolecular electrostatic interactions with  $V_{ij}$  measuring the interaction between molecules on site  $i$  and  $j$  when both molecules are in a zwitterionic state. In the following, we will only account for nearest neighbor interactions, even if extending the calculation to more general forms of the electrostatic potential is trivial. Moreover, we will impose periodic boundary conditions and will consider systems with just one molecule per unit cell. Finally, for the sake of simplicity, we will consider aligned molecules, so that only two limiting structures are of interest, as shown in Fig. 2. Since intermolecular interactions are attractive and repulsive in the two structures we dub them as J and H-structures, respectively.

Essential state models are traditionally parametrized from a detailed analysis of optical spectra (typically absorption and fluorescence) collected in solvents of different polarity, as to disentangle the effect of environmental polarity, but fully accounting for the environmental polarizability.<sup>35,36,42,44</sup> Under the assumption that the environmental polarizability (as measured e.g. by the medium refractive index) is similar in all organic media, the resulting effective model should properly account for the *core* polarizability of the surrounding molecules in the aggregate, i.e. of the polarizability due to the electronic degrees of freedom not explicitly included into the molecular essential state model. Extracting the same information from quantum chemical calculations is possible, but gas-phase results must be properly corrected to account for the environmental polarizability.<sup>45</sup>

## 2.1 Rotating the basis

The Hamiltonian in Eq.1 can be written on the basis obtained as the direct product of the  $2^N$  electronic basis states times the states (at least the first few states) of each molecular harmonic oscillator. Even accounting for just 5 vibrational states on each oscillator, the basis, growing as  $10^N$ , explodes very fast with  $N$ . The adopted diabatic basis leads to a very simple expression for the Hamiltonian describing the aggregate, but it is not the most clever basis. Indeed we need to account for all electronic states and for a large number of vibrational states simply to be able to recover a reliable description of the molecular ground state in terms of charge distribution and equilibrium geometry.

As discussed in Ref.<sup>31</sup> the molecular electronic basis can be rotated from the diabatic to the exciton basis  $|g\rangle, |e\rangle$  via the trans-

formation:

$$\begin{aligned} |g\rangle &= \sqrt{1-\rho}|N\rangle + \sqrt{\rho}|Z\rangle \\ |e\rangle &= \sqrt{\rho}|N\rangle - \sqrt{1-\rho}|Z\rangle \end{aligned} \quad (3)$$

where the parameter  $\rho$ , comprised between 0 and 1, measures the weight of the zwitterionic state into the  $|g\rangle$  state, a measure of the molecular polarity. A clever choice sets  $\rho$  to the mean-field (mf) result: when inserted in the aggregate, each dye feels the electrostatic potential generated by the surrounding molecules, and readjusts its ground state ionicity in response to this potential. The potential in turn depends on the ionicity of the molecules, leading to a self-consistent problem, that has been solved and discussed many times.<sup>11,31,37</sup>

However, the mean field ionicity is also affected by the vibrational coupling. For each molecule, the Hellman-Feynman theorem sets the equilibrium coordinate proportional to  $\rho$  as follows (see ESI for explicit expressions):<sup>38</sup>

$$\bar{Q}_i = \sqrt{\frac{2\omega_v}{\hbar}} \frac{g}{\omega_v^2} \rho \quad (4)$$

It is convenient to move the origin of the vibrational coordinate to the equilibrium position, via a Lang-Firsov transformation of the vibrational operators:<sup>21</sup>

$$\begin{aligned} \hat{Q}_i &= \hat{Q}_i - \bar{Q}_i = \sqrt{\frac{\hbar}{2\omega_v}}(\hat{a}_i^\dagger + \hat{a}_i) \\ \hat{P}_i &= \hat{P}_i = i\sqrt{\frac{\hbar\omega_v}{2}}(\hat{a}_i^\dagger - \hat{a}_i) \end{aligned} \quad (5)$$

Applying the exciton rotation to the electronic basis and the Lang-Firsov transformation to the molecular oscillators, the Hamiltonian in Eq. 1 reads (the derivation can be found in ESI):

$$\begin{aligned} \mathcal{H} &= \hbar\Omega \sum_i \hat{n}_i + \hbar\omega_v \sum_i \left( \hat{a}_i^\dagger \hat{a}_i + \frac{1}{2} \right) \\ &- g \left[ (1-2\rho) \sum_i \hat{n}_i (\hat{a}_i^\dagger + \hat{a}_i) + \sqrt{\rho(1-\rho)} \sum_i (\hat{b}_i^\dagger + \hat{b}_i) (\hat{a}_i^\dagger + \hat{a}_i) \right] \\ &+ \sum_{i>j} V_{ij} \rho (1-\rho) \left[ (\hat{b}_i^\dagger \hat{b}_j + \hat{b}_j^\dagger \hat{b}_i) + (\hat{b}_i^\dagger \hat{b}_j^\dagger + \hat{b}_j \hat{b}_i) \right] \\ &+ (1-2\rho)^2 \sum_{i>j} V_{ij} \hat{n}_i \hat{n}_j + 2\sqrt{\rho(1-\rho)}(1-2\rho) \sum_{i>j} \hat{n}_i (\hat{b}_j^\dagger + \hat{b}_j) \end{aligned} \quad (6)$$

The Paulion operator  $\hat{b}_i^\dagger$  that creates an exciton at site  $i$ , bringing the relevant molecule from the  $|g\rangle$  state (the vacuum state) to the excited  $|e\rangle$  state. The number operator  $\hat{n}_i = \hat{b}_i^\dagger \hat{b}_i$  counts the number of excitons on site  $i$  (0 for  $g$ , 1 for  $e$  states).

The above Hamiltonian is exactly equivalent to the Hamiltonian in Eq. 1, provided  $\rho$  is fixed to the mean field value:<sup>31</sup>

$$\rho = \frac{1}{2} - \frac{z(\rho)}{2\sqrt{z(\rho)^2 + \tau^2}} \quad (7)$$



where  $z(\rho)$  measures half the energy gap between the two diabatic states that self-consistently depends on  $\rho$ :

$$z(\rho) = z_0 + (M - \epsilon_v)\rho \quad (8)$$

where  $M$  defines the Madelung energy

$$M = \frac{1}{N} \sum_{i>j} V_{ij} \quad (9)$$

that reduces to  $M = V$  when only nearest neighbor interactions are considered.

To understand the physical picture that emerges from the aggregate Hamiltonian on the rotated basis (Eq. 6), we first address the mf solution for the aggregate. To start with, for an isolated molecule in the gas phase and neglecting the vibronic coupling ( $\epsilon_v = 0$ ), the solution of the two-dimensional electronic problem is trivial and leads to the  $|g\rangle$  and  $|e\rangle$  states in Eq. 3 with  $\rho$  fixed by Eq. 7 but with  $z = z_0$ . The  $|g\rangle \rightarrow |e\rangle$  transition energy and transition dipole moment are expressed as a function of  $\rho$  as follows:<sup>34</sup>

$$\begin{aligned} \hbar\Omega &= \frac{\tau}{\sqrt{\rho(1-\rho)}} \\ \mu_{ge} &= \mu_0 \sqrt{\rho(1-\rho)} \end{aligned} \quad (10)$$

where  $\mu_0$  is the dipole moment associated with the zwitterionic state, proportional to the intramolecular D-A distance. The  $\rho(z_0)$  curves and the  $\rho$ -dependence of the transition energy and dipole moments of the isolated dye are shown in fig. 1a and 1b.

When accounting for vibronic coupling, the energies of the diabatic states acquire a  $Q$ -dependence, as shown for typical model parameters in Fig. 1c. In the adiabatic approximation, the two-dimensional electronic Hamiltonian is diagonalized for each  $Q$  to get the adiabatic potential energy curves for the  $|g\rangle$  and  $|e\rangle$  states, shown in Fig. 1d. If we are only interested in adiabatic results for the equilibrium  $Q = \bar{Q}$ , we may exploit eq. 4 and solve the self-consistent two dimensional adiabatic Hamiltonian for a system where the energy difference between the diabatic states self-consistently depends on  $\rho$  as  $2z = 2z_0 - 2\epsilon_v\rho$ .<sup>38,40</sup> While the equilibrium  $\rho$  is affected by the vibrational coupling, the  $\rho$ -dependence of the transition frequency and dipole moment is always defined by Eqs. 10, so that curves in Fig. 1b apply irrespective of the  $\epsilon_v$  value.

When the dye is inserted in the aggregate its ionicity will readjust in response to the surrounding charges. In an H-type (repulsive) geometry (fig. 2a), the ionicity of the dye in the aggregate will be lower than for the isolated dye, while in a J-type (attractive) geometry it will be higher. The calculation is easy in the mf approximation: each molecule feels the electrostatic potential generated by the surrounding molecules, each one bearing a fractional charge  $\pm\rho$  at the D/A site. The energy of the zwitterionic state is then moved with respect to the isolated molecule by a quantity  $2M\rho$ , positive and negative for H and J aggregates, respectively (see Fig 2c and 2d). The mf solution of the problem is then obtained self-consistently, setting the ionicity of the surrounding molecules equal to the ionicity of the test molecule, then regaining Eq. 7. The  $\rho(z_0)$  curves in fig. 2 (e and f) are

calculated accordingly. Of particular interest is the case of J-aggregates, where not only the molecular ionicity increases with  $M$ , as expected, but, at large enough  $M$  values, a discontinuous behavior emerges,<sup>31,38,39</sup> with sizable bistability regions. Once again, the molecular ionicity is affected by the interactions, but the  $\rho$ -dependence of the transition dipole moment and frequency are fixed as in Eq. 10.

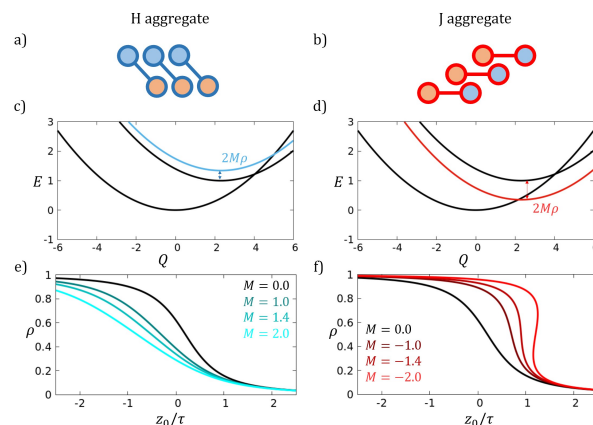


**Fig. 2** The mf dye. Panels (a) and (b) show the H and J geometries, respectively. (c) The diabatic PES for the isolated dye and for a dye in an H-aggregate. (d) The diabatic PES for the isolated dye and for a dye in a J-aggregate. (e) The  $\rho(z_0/\tau)$  curves calculated for an H aggregate with  $M=0$  (isolated dye) and  $M=1$ . (f) The  $\rho(z_0/\tau)$  curves calculated for a J aggregate with  $M=0$  (isolated dye) and  $M=-1, -1.4$  and  $-2.0$ . All results refer to systems with  $\epsilon_v = 0.4\tau$

Having described the mf solution, we are now in the position to discuss the rotated Hamiltonian in Eq. 6. The first line assigns energy  $\hbar\Omega$  to each exciton and adds the vibrational energy  $\hbar\omega_i$  to each vibrational excitation. The second line accounts for vibrational coupling. As expected, it is an on-site term. The first term in this line is the standard Condon term, with the vibrational coupling renormalized from  $g$  to  $g(1-2\rho)$  to account for the relative position of the equilibrium geometries for the ground and excited state potential energy surfaces (PES).<sup>46</sup> The second term in the second line is instead an ultraexcitonic term mixing states with the number of excitons differing by one unit. This ultraexciton term has a vibronic origin: the creation/destruction of the exciton on site  $i$  is always accompanied by the creation or destruction of a vibrational quantum in the same site. The terms in the two last lines of Eq. 6 all come from intermolecular electrostatic interactions. The term in the third line is proportional to the squared transition dipole moment of the mf dye (see eq. 10) and contains both the exciton hopping term, as well as the two-exciton terms that are usually neglected in the exciton model.<sup>25</sup> In the last line the first term is an exciton-exciton interaction term (proportional to the squared mesomeric moment): it conserves the exciton number and it may enter the exciton model, but is of course relevant only to aggregates of polar dyes.<sup>31</sup> The very last term is again an ultraexcitonic term mixing states whose exciton number changes by one unit.

A special situation occurs in the so-called cyanine limit, when the mean field  $\rho$  attains the 0.5 value. This occurs whenever

$z(\rho = 0.5) = 0$  in Eq. 8, or  $2z_0 - \varepsilon_v = M$  ( $2z_0 - \varepsilon_v = V$ , for nearest neighbor interactions), fully in line with the analogous result for a dimeric aggregate in Ref. <sup>43</sup>. In the cyanine limit, the leading Condon term for vibronic coupling vanishes, and the vibronic structure in aggregate spectra is washed out,<sup>43</sup> with marginal vibronic effects only expected for strong coupling, when the ultraexcitonic term enters into play. Moreover, all excitonic and ultraexcitonic terms proportional to  $(1 - 2\rho)$  (i.e. to the mesomeric dipole moment) vanish when  $\rho = 0.5$  so that only terms proportional to the squared transition dipole moment survive. In the cyanine limit then the electronic part of the Hamiltonian in Eq. 6 reduces to the Hamiltonian for aggregates of non-polar dyes.<sup>25</sup>

## 2.2 Computational strategy

The dimension of the non-adiabatic basis increases fast with the aggregate dimension. On each molecular unit the basis includes 2 electronic states to be multiplied by the number of vibrational states as needed for convergence  $n_{ph}$ . The basis for an aggregate of  $N$  molecules has then dimension  $(2n_{ph})^N$ , quickly leading to untractable problems. To overcome this limitation, we make use of symmetry: the adopted periodic boundary conditions in fact not only help minimizing finite size effects, but also enforce translational symmetry in the system. The wavevector  $k$  is then a good quantum number for the aggregate, with optical transitions obeying a strict selection rule imposing that only states with the same wavevector can be reached. The ground state is a zero-wavevector state, so that only the  $k = 0$  subspace is of interest for absorption processes. In J-aggregates the lowest excited state also has  $k = 0$ , so that, again, only the  $k = 0$  subspace is of interest. In H-aggregates instead the lowest excited state belongs to the  $k = \pi$  subspace, so that, to address fluorescence in H-aggregates, we must also diagonalize the model Hamiltonian in the  $k = \pi$  subspace.

To further reduce the dimension of the problem we work in the exciton basis that, while leading to a fairly cumbersome Hamiltonian, allows, for not too large intermolecular interactions, to limit the basis dimension discarding all states with a number of excitations larger than  $M_e$  with  $M_e \leq N$ . Moreover, we truncate the vibrational basis as to discard all states with a total number of vibrational quanta larger than  $M_v$ . Of course, large enough  $M_e$  and  $M_v$  must be considered to ensure convergence on relevant results.

In the bit-representation, we store each basis state in the computer memory as an integer number whose binary code is composed of 4 bits for each molecule in the aggregate, where the first bit represents the electronic state ( $0 \equiv |g\rangle$ ,  $1 \equiv |e\rangle$ ) and the following 3 bits store the integer number that counts the vibrational quanta (from a minimum of  $000 \equiv |0\rangle$  to a maximum of  $111 \equiv |7\rangle$ ). The basis set is created scrolling through all integer numbers from 0 to  $16^{N-1}$  and selecting only the states that comply with the required values of  $M_e$  and  $M_v$ . Translational symmetry operations are then applied to the basis states to finally obtain symmetry-adapted linear combinations in the  $k = 0$  space, as needed to calculate spectra of J and H-aggregates, and in the  $k = \pi$  subspace for H-aggregates to address their fluorescence spectra. Since the basis is very large, we only store a single representative state for

each symmetry-adapted linear combination, together with the information concerning its multiplicity. The Hamiltonian in Eq. 6 is finally written on the symmetrized basis and diagonalized in the relevant subspaces. Depending on the number of excitons and vibrational states needed to reach convergence, we are able to address systems with up to  $N = 6$  sites (of course only aggregates with an even  $N$  can be considered in the  $k = \pi$  subspace).

## 3 Results

In the following we set  $\tau = 1$ , as the energy unit (typical values for CT dyes are of the order of 1 eV, even if for dyes of interest for thermally activated delayed fluorescence<sup>47</sup>  $\tau$  can be up to an order of magnitude smaller), and fix  $\varepsilon_v = 0.4$  and  $\omega_v = 0.17$ . Results will be shown for different  $z_0$  as to describe the properties of dyes with different ionicities. All results were obtained setting  $N_v = 6$ .

### 3.1 Weak coupling

We start our analysis with H-aggregates, setting a moderate value for the electrostatic interaction,  $V = 1$ . Fig. 3 shows results for a largely neutral dye, a dye with intermediate ionicity and a zwitterionic dye. Results are shown for the biggest achievable aggregate  $N=6$ , but finite size effects are negligible in this case. Convergence is obtained already for  $N_e=3$ , as the  $N_e = 3$  and 4 results are superimposed in the scale of the figure. In all cases, in line with the H-nature of the aggregate, as determined by repulsive intermolecular interactions, the fluorescence intensity is largely suppressed as a result of aggregation, and a huge Stokes shift is observed for the aggregate. Understanding the position of absorption bands is however tricky. With reference to the isolated (gas phase) dye, the absorption band blueshifts for the dyes with low and intermediate polarity (left and central panels), but red-shifts in the case of a largely polar dye (right panel). These apparently crazy results, possibly suggesting the failure of the exciton picture, are indeed related to a bad choice of the reference state. A large part of the shift in fact is not excitonic in origin, but is related to the effects that surrounding charges have on the energy of the states. This is easily calculated in the mf approximation. Repulsive intermolecular interactions reduce the polarity of each dye in the aggregate (see fig. 2e), hence affecting the frequency of the absorption band. The proper reference for the exciton model is indeed represented by the mf absorption frequency. Specifically, for the dye in the left panels of Fig. 3, the ionicity decreases from 0.19 in the gas phase to a mf value of 0.17. Accordingly, the maximum of the absorption blueshifts, slightly reducing the exciton shift. Similar considerations apply to the dye in the middle panels, whose ionicity is reduced from 0.64 in the gas phase to 0.5 in the mf approach. For  $\rho = 0.5$  (the cyanine limit) the Condon vibrational coupling (proportional to the squared mesomeric dipole moment) vanishes, leading to the disappearance of the vibronic structure in absorption and fluorescence bands. More inspiring is the case of the zwitterionic dye in right column of Fig. 3. Here the decrease of the ionicity from 0.76 in the gas phase to 0.61 in the mf approximation is responsible for a large red-shift of the absorption band. Taking as proper reference the mf frequency, a blue-shift of the absorption band is observed for the aggregate,

fully in line with its H character, as due to repulsive ( $V > 0$ ) intermolecular interactions.

Fluorescence in H-aggregates comes from electronic states at the border of the Brillouin zone and are therefore only allowed due to the coupling to vibrational modes. As a result, very weak and largely red-shifted bands are observed, but what we notice here is that, since the dominating (Condon) term accounting for vibronic coupling vanishes in the cyanine limit, the fluorescence intensity is vanishingly small in this limit.

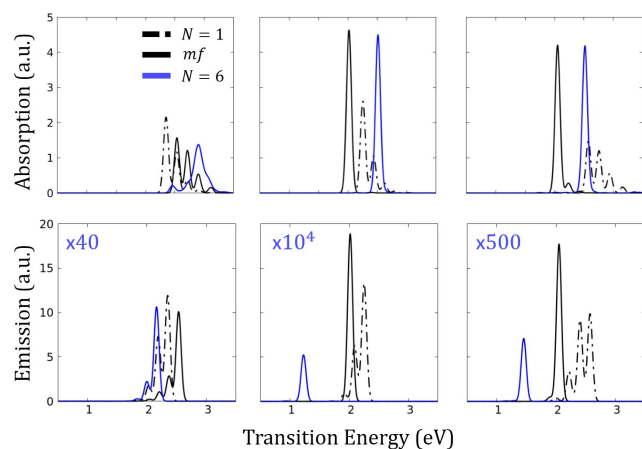


**Fig. 3** H aggregate,  $V=1$ ,  $\epsilon_v=0.4$ ,  $\omega_v=0.17$ : top and bottom panel show calculated absorption and fluorescence spectra. Intensities per molecules are reported in arbitrary units. The weak fluorescence spectra of the aggregate are multiplied by a factor, as shown in the figure. Left panels refer to a system with  $z_0=0.8$ , corresponding to an ionicity for the isolated dye  $\rho=0.21$  that decreases in the mf approximation to  $\rho=0.17$ . Middle panels:  $z_0=-0.3$ , gas phase  $\rho=0.76$ , mf  $\rho=0.5$ . Right panels:  $z_0=-0.6$ , gas phase  $\rho=0.84$ , mf  $\rho=0.61$ .

A similar analysis applies to the aggregates in Fig. 4, corresponding to the case of weak attractive intermolecular interactions ( $V = -1$ ). Intense emission bands and vanishing Stokes shifts in the aggregate are fully in line with J-aggregate behavior. The redshift of absorption (and emission) bands observed for the dyes in the left and middle panels of Fig. 4 are again in line with a J-aggregate behavior. The most striking results is however recognized again for the most polar molecule ( $\rho = 0.36$  in the gas phase) in the right panels of Fig. 4: here in fact the exciton band moving to the blue with respect to the gas-phase molecule. But again this anomalous behavior is simply related to the choice of a wrong reference. In the aggregate, the mf solution of the problem drives the molecule deep in the ionic regime with  $\rho = 0.82$ . This implies a large blue shift of the absorption and fluorescence bands, so that, when taking as reference the gas phase molecule, an apparent blue-shift of the exciton band is observed, that actually corresponds to a red-shift when the proper mf reference is considered, in line with the attractive nature of the interactions. We also notice that for the zwitterionic system, when the wrong reference state is considered, the intensity of the transitions (both absorption and fluorescence) decreases and the vibronic structure becomes more prominent, in striking contrast with the J-nature of the aggregate. This inconsistency is however

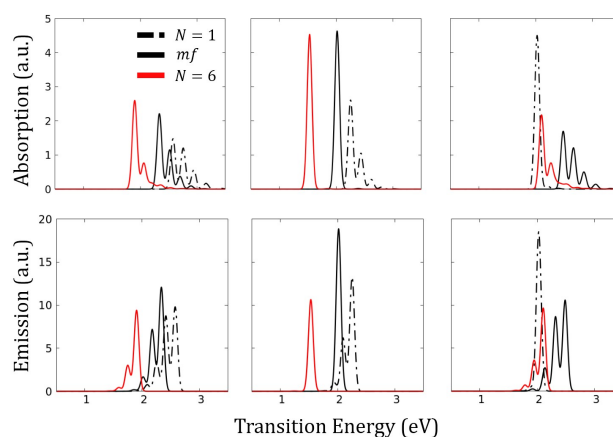


**Fig. 4** J aggregate,  $V=-1$ ,  $\epsilon_v=0.4$ ,  $\omega_v=0.17$ : top and bottom panel show calculated absorption and fluorescence spectra. Intensities per molecules are reported in arbitrary units. Left panels refer to a system with  $z_0=1.0$ , corresponding to an ionicity for the isolated dye  $\rho=0.15$  that increases in the mf approximation to  $\rho=0.21$ . Middle panels:  $z_0=0.7$ , gas phase  $\rho=0.21$ , mf  $\rho=0.50$ . Right panels:  $z_0=0.3$ , gas phase  $\rho=0.36$ , mf  $\rho=0.82$ .

quite naturally solved if the proper mf reference is considered: in all cases the spectral intensity increases when going from the mf dye to the aggregate, while the vibronic structure becomes less and less prominent. Quite interestingly, results in the central panel of Fig. 4 refer to a dye with ionicity  $\rho = 0.16$  in the gas phase that is driven to the cyanine limit,  $\rho = 0.50$  when embedded in the aggregate. Once again, in the cyanine limit the vibronic structure of absorption and fluorescence bands disappears.

### 3.2 Medium and strong coupling

We will now address the cases of medium and strong coupling. Fig. 5 shows absorption spectra calculated for H-aggregates in the medium ( $V = 1.6$ ) and strong-coupling ( $V = 2.0$ ) regimes. It turns out that  $N_e = 4$  is the minimum number of exciton states to be introduced to get convergence,  $N_e = 3$  results are totally untenable, with the only exception of the systems that in the mf approximation have  $\rho = 0.5$ . In these conditions in fact all terms in Eq. 6 proportional to  $1 - 2\rho$  vanish. Accordingly, the vibronic structure disappears, as discussed above, but also all terms related to the mesomeric dipole moment (the difference between the permanent dipole moments in the excited and ground state) vanish. For the electronic part, the Hamiltonian in the  $\rho = 0.5$  limit reduces to that relevant to a non-polar aggregates and most of the anomalous effects associated with aggregates of polar and polarizable dyes are washed out.<sup>43</sup> Once convergence is reached, finite size effects are marginal for largely neutral dyes, as well as for dyes in the cyanine limit, but become relevant for zwitterionic dyes.

More interesting is the case of J-aggregates, where electrostatic intermolecular interactions lead to intriguing phenomena.<sup>31,32</sup> Fig. 6 shows absorption and fluorescence spectra calculated for a system with  $V=-1.6$ , corresponding to the curve in Fig. 2f that marks the boundary between the normal (weak coupling) and the bistable (strong coupling) regime. Much as in the weak cou-



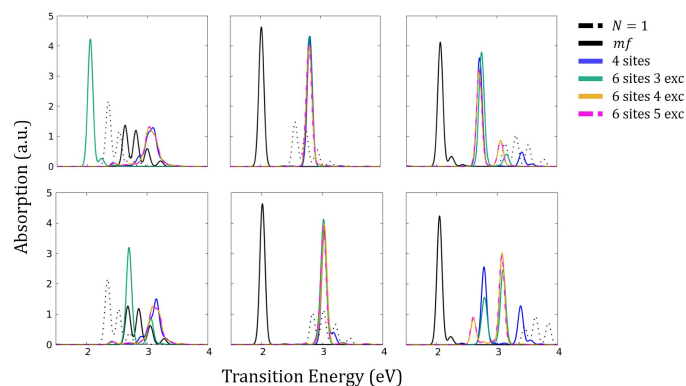


**Fig. 5** H aggregate absorption spectra. All results refer to a system with  $\epsilon_v = 0.4$  and  $\omega_v = 0.17$ . Top panels show results for  $V = 1.6$ , from left to right:  $z_0 = 0.8$ , gas phase  $\rho = 0.21$ , mf  $\rho = 0.15$ ;  $z_0 = -0.6$ , gas phase  $\rho = 0.84$ , mf  $\rho = 0.5$ ;  $z_0 = -1.0$ , gas phase  $\rho = 0.9$ , mf  $\rho = 0.62$ . Bottom panels show results for  $V = 2.0$ , from left to right:  $z_0 = 0.8$ , gas phase  $\rho = 0.21$ , mf  $\rho = 0.14$ ;  $z_0 = -0.8$ , gas phase  $\rho = 0.88$ , mf  $\rho = 0.5$ ;  $z_0 = -1.2$ , gas phase  $\rho = 0.92$ , mf  $\rho = 0.61$ .

pling case, the apparently anomalous behavior observed when comparing aggregate spectra with spectra calculated for the isolated dye are relieved if the proper reference system is considered, corresponding to the mf solution. In all cases in fact the aggregate spectrum is red-shifted with respect to the relevant mf spectrum. The most important difference with respect to the weak coupling is the appearance of finite size effects, with  $N=6$  results differing from  $N=4$ , pointing to largely delocalized excitons. Moreover, to get convergence for  $N=6$  at least  $N_e=4$  is needed (see Fig. S1) in sharp contrast with the weak coupling case. Quite interestingly, finite size effects are marginal for the system described in middle column of fig. 6 where the mf ionicity is 0.5. As discussed above, in this limit, the vanishing of terms proportional to  $1 - 2\rho$  not only kills the main vibronic coupling term, but also reduces the electronic part of the Hamiltonian to that of aggregates of non-polar dyes.

This is even more evident in the strong coupling limit in fig. 7, showing spectra calculated for  $V = -2.0$ . Similar considerations apply as in the medium-coupling regime, but in this case  $N = 6$  results do not converge until the maximum number of excitons  $N_e = 6$  is accounted for in the calculation, or in other terms, the complete electronic basis is considered (see fig S2). This immediately tells us that the exciton-exciton interaction term (the first term in the last line of Eq. 6, lowers the energy of multiexciton states that get mixed with the lowest excited states giving a sizable multiexcitonic character to the state, as extensively discussed in refs.<sup>31,32</sup> Again, this term vanishes for a system with a mf ionicity  $\rho = 0.5$ , so that for this system (middle panel of fig. 7) the  $N=6$  results already converge at  $N_e = 3$ .

## 4 Discussion

Extending a previous work<sup>31</sup> to account for molecular vibrations, as needed to properly address spectral bandshapes, here we propose a two-step approach to the description of optical spectra of aggregates of polar and polarizable molecules. The first step is

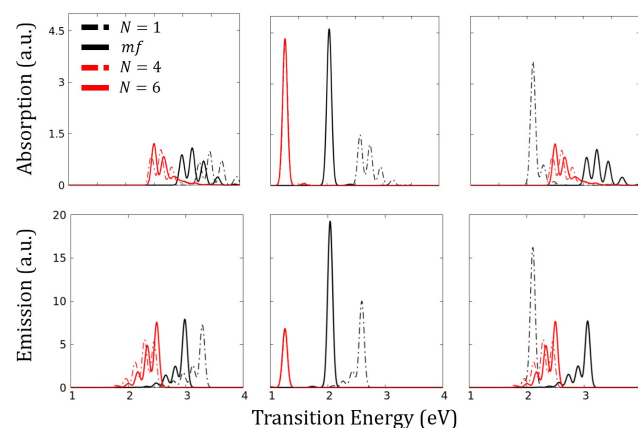


**Fig. 6** J aggregate,  $V = -1.6$ ,  $\epsilon_v = 0.4$ ,  $\omega_v = 0.17$ : top and bottom panel show calculated absorption and fluorescence spectra. Intensities per molecule are reported in arbitrary units. Left panels refer to a system with  $z_0 = 1.5$ , corresponding to an ionicity for the isolated dye  $\rho = 0.09$  that increases in the mf approximation to  $\rho = 0.10$ . Middle panels:  $z_0 = 1.0$ , gas phase  $\rho = 0.16$ , mf  $\rho = 0.50$ . Right panels:  $z_0 = 0.5$ , gas phase  $\rho = 0.33$ , mf  $\rho = 0.90$ .

the definition of the proper reference state as the mf solution of the problem. Basically, the ground state polarity of each dye is self-consistently defined by the polarity of the surrounding dyes, leading to increased polarity for attractive intermolecular interactions and reduced polarity for repulsive interactions. Of course all molecular properties (including transition frequencies and dipole moments) are affected by this variation. The mf state defines the proper reference state for the exciton model. The molecular geometry is also affected by the molecular polarity and the correct reference state for the vibrational problem is defined via a Lang-Firsov transformation that translates the origin of the vibrational coordinates to the equilibrium position relevant to the charge distribution of the molecule inside the aggregate. Since molecular vibrations in turn affect the molecular polarity, vibronic coupling leads to another self-consistent interaction. While this may look as a difficult problem, it boils down to a simple self-consistent diagonalization of a two by two Hamiltonian.<sup>39,42</sup>

The essential state model adopted here has been extensively validated against experiment and describes in a very effective way the low-energy spectral properties of push-pull dyes accounting for environmental effects in solution,<sup>34–36</sup> aggregates,<sup>33,42</sup> films<sup>44</sup> and crystals.<sup>39,48</sup> In the context of this work we underline that the model relies on similar approximations as the standard exciton model, accounting for a single electronic excitation and a single vibrational mode per molecule. At variance with the standard exciton model, however, the proposed model fully accounts for the molecular polarizability and for the dependence of the ground and excited state molecular geometry on the molecular polarity.

Once the proper reference state is defined, several interaction terms are recognized in the Hamiltonian that can be classified as excitonic, when conserving the exciton number, and ultraexcitonic when mixing states with a different number of excitons.<sup>31</sup> The vibrational coupling leads to an excitonic term that corre-

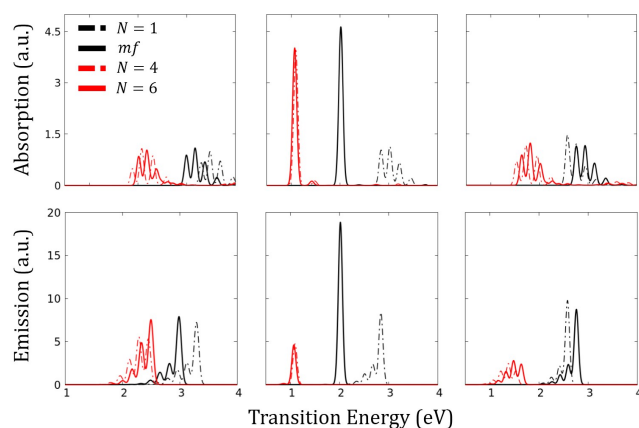


**Fig. 7** J aggregate,  $V=-2.0$ ,  $\varepsilon_v=0.4$ ,  $\omega_v=0.17$ : top and bottom panel show calculated absorption and fluorescence spectra. Intensities per molecules are reported in arbitrary units. Left panels refer to a system with  $z_0=1.5$ , corresponding to an ionicity for the isolated dye  $\rho=0.09$  that increases in the mf approximation to  $\rho=0.11$ . Middle panels:  $z_0=1.2$ , gas phase  $\rho=0.12$ , mf  $\rho=0.50$ . Right panels:  $z_0=1.0$ , gas phase  $\rho=0.16$ , mf  $\rho=0.87$ .

sponds to the Condon coupling in the exciton model. This term is proportional to  $1-2\rho$ , and vanishes in systems whose mf ionicity is close to 0.5: in these systems the vibronic bands shape is washed out. The ultraexcitonic term exchanges vibrational quanta and excitons and has marginal spectroscopic effects in the weak coupling limit as shown in Fig. 8 and 9 that compare exact results obtained in the weak and strong coupling regimes for H and J aggregates with those obtained suppressing the non-Condon vibronic coupling in the Hamiltonian in Eq. 6. Non-Condon corrections give rise to sizable effects in the strong regime.

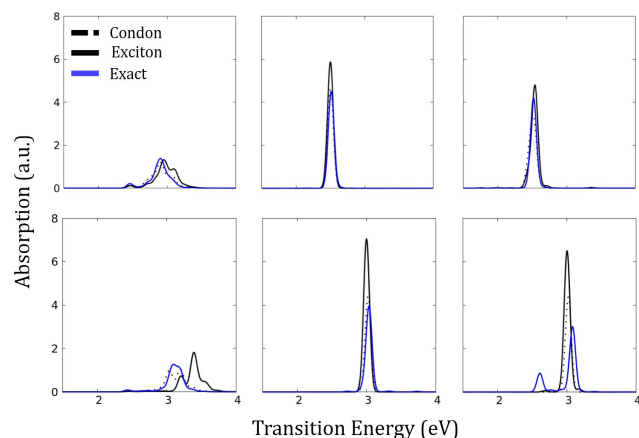


**Fig. 8** H aggregates with  $N=6$ . Top panel show weak-coupling results,  $V=1$  for the same values of model parameters as in Fig. 3; bottom panels show results for strong coupling,  $V=2$ , for the same parameters as in the bottom panels of Fig. 5. In all panels blue lines show converged results for the total Hamiltonian, dashed black curves show results obtained neglecting the non-Condon electron-vibration coupling term, continuous black lines show results for the exciton model, i.e. suppressing all ultraexcitonic terms in the Hamiltonian.

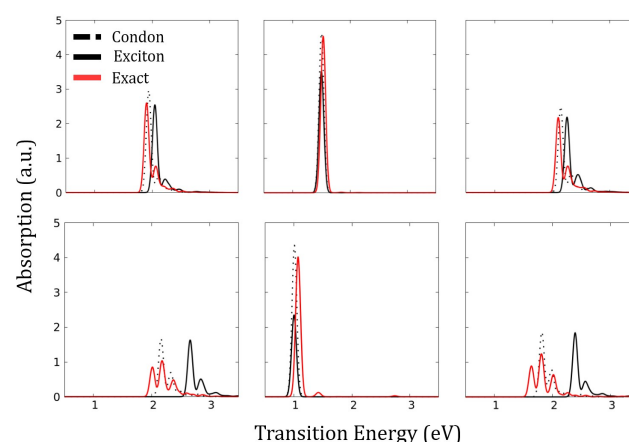


**Fig. 9** J aggregates with  $N=6$ . Top panel show weak-coupling results,  $V=-1$  for the same values of model parameters as in Fig. 4; bottom panels show results for strong coupling,  $V=-2$ , for the same parameters as in Fig. 7. In all panels blue lines show converged results for the total Hamiltonian, dashed black curves show results obtained neglecting the non-Condon electron-vibration coupling term, continuous black lines show results for the exciton model, i.e. suppressing all ultraexcitonic terms in the Hamiltonian.

As for excitonic terms originating from electrostatic interactions, we recognize terms  $\propto \rho(1-\rho)$ , i.e. proportional to the squared transition dipole moment of the mf molecules: these terms are responsible for the exciton hopping. Other terms appear proportional to the mesomeric dipole moment  $(1-2\rho)$  that account for exciton-exciton interactions. These last terms vanish when the mf molecular ionicity is close to 0.5, and the system reduces to an aggregate of non-polar dyes. The exciton approximation works reasonably well for weak coupling, but fails in the strong coupling regimes (see fig. 8 and 9).

Indeed, with increasing coupling, ultraexciton terms enter into play with particularly impressive effects in J-aggregates, where bistability regions are observed in the mf solution.<sup>31,32</sup> Finite size effects become important in these conditions and the exciton basis cannot be broken down to account for just the first few exciton states (up to 3 excitons are enough to get converged results in the weak coupling limit). Indeed, the lowest excited state in these conditions cannot be described, not even approximately, as a state with a single exciton, rather it corresponds to a state where several excited molecules cluster together in a multiexciton state.<sup>31,32</sup>

In this work we only consider perfectly ordered 1D aggregates. Accordingly, translational symmetry is exploited to successfully address the fairly complex problem of coupled electronic and vibrational motion in fairly large systems. Modest disorder effects are expected in crystalline systems, but they are important for aggregates in solution. Molecular dynamics and more generally multiscale approaches are powerful tools to address disorder that in aggregates in solution<sup>49,50</sup> as related to the conformational motion of the aggregate itself, as well as to fluctuating electric field associated with polar solvation. However, treating electronic and vibrational degrees of freedom in a truly non-adiabatic ap-

proach is challenging for large disordered systems, and requires the development of new approximation techniques. In this respect, the proposed two-step approach to aggregates of polar dyes may offer a good starting point towards the development of few-particle approaches, that are successfully exploited for aggregates of non-polar dyes.<sup>7,17,22,25</sup>

## 5 Conclusions

Spectroscopic effects of intermolecular interactions have attracted the interest of scientists since almost a century. The exciton model, neglecting intermolecular interactions among non-degenerate states, offers a simple and effective approach to understand spectral properties of molecular crystals and aggregates.<sup>7,14,15</sup> However, it must be recognized that the model fully neglects the molecular polarizability,<sup>31</sup> in the assumption that the nature of the ground state is not altered by intermolecular interactions. This approximation works fairly well in aggregates of non-polar molecules, where the molecular polarizability shows up mainly with a variation of the spectral intensities,<sup>25</sup> an effect that is difficult to assess experimentally. In aggregates of polar molecules, however, the large electric fields generated by the nearby polar molecules considerably affect the state of polarizable dyes leading to two major effects. In the first place, when a polar and polarizable molecule is surrounded other similar molecules, it will readjust its polarity in response to the electrical potential generated by the charges in the surrounding molecules. Accordingly, the nature of the molecules will change, with the ground state polarity at equilibrium being reduced in H aggregates with respect to the isolated molecule and increased in J-aggregates. Of course, the equilibrium geometry of the molecule will readjust accordingly. To properly rationalize aggregation effects it is important to take in proper account this mean-field effect, building the model for interacting dyes starting from the proper reference. This allows to single out excitonic and ultraexcitonic effects and to properly address vibrational coupling and hence vibronic band-shapes. Specifically, the anomalous red/blue shifts observed in H/J aggregates when the reference state is taken to correspond to the isolated molecule, turn out to be normal blue/red shifts when the proper reference is taken as the molecule in its environment. Similar anomalous effects on band-shapes are also easily sorted out, at least in the weak-coupling regime. Apart from a better understanding of the physics of these intriguing systems, the proper choice of the reference state gives an enormous computational advantage: for not too large couplings in fact it is possible to truncate the electronic basis only accounting for states with a limited number of excitons. This is particularly important because the non-adiabatic basis, needed to properly address the aggregate, increases very fast with the number of states. Our approach, that also accounts for the translational symmetry in aggregates with periodic boundary conditions, allowed us to diagonalize exactly the non-adiabatic Hamiltonian for systems with up to 6 molecules. Reaching large aggregates is important to single out finite size effects that are particularly interesting for J-aggregates in the medium-large coupling regime, where the low-lying excitations acquire a multiexciton character, corresponding to a droplet of excited states bound together by attractive inter-

molecular interactions. In this paper we only considered linear absorption and fluorescence spectra, but our approach can easily address non-linear optical spectra, where important aggregation effects are expected.

## Conflicts of interest

There are no conflicts to declare.

## Acknowledgements

This project received funding from the European Union Horizon 2020 research and innovation programme under Grant Agreement No. 812872 (TADFlife), and benefited from the equipment and support of the COMP-HUB Initiative, funded by the “Departments of Excellence” program of the Italian Ministry for Education, University and Research (MIUR, 2018-2022). We acknowledge the support from the HPC (High Performance Computing) facility of the University of Parma, Italy.

## Notes and references

- 1 Förster, Th., *Modern Quantum Chemistry*, Academic Press, 1965, p. 93.
- 2 Scholes, G. D., *Annu. Rev. Phys. Chem.*, 2003, **54**, 57–87.
- 3 Di Maiolo, F. and Painelli, A., *J. Chem. Theory Comput.*, 2018, **14**, 5339–5349.
- 4 M. Anzola, C. Sissa, A. Painelli, A. A. Hassanali and L. Grisanti, *Journal of Chemical Theory and Computation*, 2020, **16**, 7281–7288.
- 5 Craig, D. P. and Walmsley, S. H., *Excitons in Molecular Crystals*, Benjamin, 1968.
- 6 Knoester, J., *Organic Nanostructures: Science and applications*, IOS Press, Amsterdam, 2002, vol. 149, pp. 149–186.
- 7 Hestand, N. J. and Spano, F. C., *Chem. Rev.*, 2018, **118**, 7069–7163.
- 8 Lakowicz, J. R., *Principles of Fluorescence Spectroscopy*, Springer US, 1999, p. 698.
- 9 B. Valeur and M. N. Berberan-Santos, *Molecular Fluorescence: Principles and Applications*, Wiley-VCH Verlag GmbH & Co. KGaA, 2012.
- 10 Rice, M. J., *Phys. Rev. Lett.*, 1976, **37**, 36–39.
- 11 Painelli, A. and Girlando, A., *J. Chem. Phys.*, 1986, **84**, 5655–5671.
- 12 M. Souto, J. Guasch, V. Lloveras, P. Mayorga, J. T. L. Navarrete, J. Casado, I. Ratera, C. Rovira, A. Painelli and J. Veciana, *The Journal of Physical Chemistry Letters*, 2013, **4**, 2721–2726.
- 13 N. J. Hestand, C. Zheng, A. R. Penmetcha, B. Cona, J. A. Cody, F. C. Spano and C. J. Collison, *The Journal of Physical Chemistry C*, 2015, **119**, 18964–18974.
- 14 Kasha, M., *Radiat. Res.*, 1964, **3**, 317–331.
- 15 Davidov, A. S., *Theory of Molecular Excitons*, Plenum Press, 1971.
- 16 Agranovich, V. M. and Galanin, M. D., *Excitons in Molecular Crystals*, North-Holland, 1982.
- 17 Spano, F. C., *Acc. Chem. Res.*, 2010, **43**, 429–439.
- 18 E. U. Condon, *Reviews of Modern Physics*, 1937, **9**, 432–457.

- 19 D. P. Craig and T. Thirunamachandran, *Molecular quantum electrodynamics*, Dover, New York, NY, 1998.
- 20 K. Swathi, C. Sissa, A. Painelli and K. G. Thomas, *Chemical Communications*, 2020, **56**, 8281–8284.
- 21 Feinberg, D. and Ciuchi, S. and De Pasquale, F., *Int. J. Mod. Phys. B*, 1990, **04**, 1317–1367.
- 22 Hoffmann, M. and Soos, Z. G., *Phys. Rev. B*, 2002, **66**, 024305.
- 23 Spano, F. C. and Yamagata, H., *J. Phys. Chem. B*, 2011, **111**, 5133–5143.
- 24 Painelli, A., *Chemical Physics*, 1999, **245**, 185 – 197.
- 25 M. Anzola, F. D. Maiolo and A. Painelli, *Physical Chemistry Chemical Physics*, 2019, **21**, 19816–19824.
- 26 D'Avino, G. and Terenziani, F. and Painelli, A., *ChemPhysChem*, 2007, **8**, 2433–2444.
- 27 Sanyal, S. and Painelli, A. and Pati, S. K. and Terenziani, F. and Sissa, C., *Phys. Chem. Chem. Phys.*, 2016, **18**, 28198–28208.
- 28 Bardi, B. and Dall'Agnese, C. and Moineau-Chane Ching, K. I. and Painelli, A. and Terenziani, F., *J. Phys. Chem. C*, 2017, **121**, 17466–17478.
- 29 Zheng, C. and Zhong, C. and Collison, C. J. and Spano, F. C., *J. Phys. Chem. C*, 2019, **123**, 3203–3215.
- 30 Bardi, B. and Dall'Agnese, C. and Tassé, M. and Ladeira, S. and Painelli, A. and Moineau-Chane Ching, K. I. and Terenziani, F., *ChemPhotoChem*, 2018, **2**, 1027–1037.
- 31 Terenziani, F. and Painelli, A., *Phys. Rev. B*, 2003, **68**, 165405.
- 32 A. Painelli and F. Terenziani, *Journal of the American Chemical Society*, 2003, **125**, 5624–5625.
- 33 Terenziani, F. and D'Avino, G. and Painelli A., *ChemPhysChem*, 2007, **8**, 2433–2444.
- 34 Painelli, A., *Chemical Physics Letters*, 1998, **285**, 352 – 358.
- 35 Painelli, A. and Terenziani, F., *The Journal of Physical Chemistry A*, 2000, **104**, 11041–11048.
- 36 Boldrini, B. and Cavalli, E. and Painelli, A. and Terenziani, F., *The Journal of Physical Chemistry A*, 2002, **106**, 6286–6294.
- 37 Soos, Z. G. and Klein, D. J., in *Molecular Association: Including Molecular Complexes*, Vol. 1, Academic Press, New York, 1975.
- 38 A. Girlando and A. Painelli, *Physical Review B*, 1986, **34**, 2131–2139.
- 39 J. Guasch, L. Grisanti, S. Jung, D. Morales, G. D'Avino, M. Souto, X. Fontrodona, A. Painelli, F. Renz, I. Ratera and J. Veciana, *Chemistry of Materials*, 2013, **25**, 808–814.
- 40 G. D'Avino, A. Painelli and Z. Soos, *Crystals*, 2017, **7**, 144.
- 41 F. Terenziani and A. Painelli, *Journal of Luminescence*, 2005, **112**, 474–478.
- 42 Sanyal, S. and Sissa, C. and Terenziani, F. and Pati, S. K. and Painelli, A., *Phys. Chem. Chem. Phys.*, 2017, **19**, 24979–24984.
- 43 C. Zhong, D. Bialas and F. C. Spano, *The Journal of Physical Chemistry C*, 2020, **124**, 2146–2159.
- 44 Terenziani, F. and Painelli, A. and Girlando, A. and Metzger, R. M., *The Journal of Physical Chemistry B*, 2004, **108**, 10743–10750.
- 45 D. K. A. P. Huu, C. Sissa, F. Terenziani and A. Painelli, *Physical Chemistry Chemical Physics*, 2020, **22**, 25483–25491.
- 46 A. Painelli and F. Terenziani, *Chemical Physics Letters*, 1999, **312**, 211 – 220.
- 47 H. Nakanotani, T. Higuchi, T. Furukawa, K. Masui, K. Morimoto, M. Numata, H. Tanaka, Y. Sagara, T. Yasuda and C. Adachi, *Nature Communications*, 2014, **5**, 4061.
- 48 G. D'Avino, L. Grisanti, J. Guasch, I. Ratera, J. Veciana and A. Painelli, *Journal of the American Chemical Society*, 2008, **130**, 12064–12072.
- 49 A. Segalina, X. Assfeld, A. Monari and M. Pastore, *The Journal of Physical Chemistry C*, 2019, **123**, 6427–6437.
- 50 M. Eskandari, J. C. Roldao, J. Cerezo, B. Milián-Medina and J. Gierschner, *Journal of the American Chemical Society*, 2020, **142**, 2835–2843.